Design-Oriented Modeling of Nonlinear Structures

Session Organizer: Bassam IZZUDDIN (Imperial College)

Keynote Lecture
Simplified modeling of nonlinear structures – "Spanning component to system"
Bassam A. IZZUDDIN (Imperial College)

Limit analysis of slabs revisited with finite element models
Edward MAUNDER, Angus RAMSAY (University of Exeter)*

Effects of boundary conditions on the non-linear long-term behavior of spherical shallow concrete domes
Ehab HAMED, Mark A. BRADFORD, R. Ian GILBERT (University of New South Wales)*

A local failure model for shallow spherical concrete domes subjected to uniform external radial pressure
Zhen-Tian CHANG, Mark A. BRADFORD, R. Ian GILBERT (University of New South Wales)*

For multiple-author papers:
Contact author designated by *
Presenting author designated by underscore

Proceedings of the 6th International Conference on
Computation of Shell and Spatial Structures
IASS-IACM 2008: "Spanning Nano to Mega"
28-31 May 2008, Cornell University, Ithaca, NY, USA
John F. ABEL and J. Robert COOKE (eds.)

Simplified modeling of nonlinear structures – "Spanning component to system"

Bassam A. IZZUDDIN

Imperial College London
Department of Civil and Environmental Engineering,
Imperial College London, London, SW7 2AZ, UK
Email: b.izzuddin@imperial.ac.uk

Abstract

This paper discusses the role of simplified modelling in nonlinear structural analysis, addressing a range of structural forms from individual components to overall systems. The principal benefits of simplified modelling are identified as i) ease of application, ii) adequacy for preliminary assessment, iii) sufficiency in the presence of uncertainty in structure and/or load, and iv) explicit cause-and-effect formulation leading to enhanced understanding and appreciation of the main parameters influencing the nonlinear structural response. The aforementioned benefits are demonstrated with three examples of simplified nonlinear modelling, namely i) a simplified SDOF model for steel members subject to fire and blast loading, ii) simplified buckling analysis using a rotational spring analogy, and iii) simplified progressive collapse assessment of multi-storey buildings.

1. Introduction

Recent years have witnessed an increased need for nonlinear structural analysis in the design and assessment of structures. While detailed nonlinear finite element analysis has provided an essential tool towards fulfilling this need, simplified mechanical models have been widely recognised as offering important benefits that can outweigh their relative inaccuracy. These benefits include i) ease of application via hand calculation or simple computational tools such as spreadsheet programs, ii) adequacy for preliminary assessment when a rough estimate is being sought, iii) sufficiency in the presence of uncertainty in the structural details or loading characteristics, and iv) explicit cause-and-effect formulation, removing the application from the typical 'black-box' use associated with finite element analysis, and leading to enhanced understanding and appreciation of the main parameters influencing the nonlinear structural response.

Three examples of simplified modelling are presented hereafter, illustrating its applicability to a range of structural forms from individual components to overall systems, and demonstrating its aforementioned benefits.

2. Simplified Model for Steel Members Subject to Fire and Blast

A simplified model was developed by Izzuddin [3] for steel beam components subject to blast, which accounts for the elasto-plastic response, including plastic bending and catenary actions, under various support conditions (e.g. Figure 1 for simply supported beam). With the assumption of a SDOF dominant dynamic mode based on the static response (Biggs [1]), an explicit formulation is achieved (Izzuddin [3,4]), which not only is easily applied but also offers the cause-and-effect transparency that practising engineers find very useful. More recently, the static model was extended to deal with the influence of elevated temperatures (Izzuddin [4]), where an additional compressive catenary stage was identified. Despite its inherent approximating assumptions, this design-oriented model was shown to provide very good predictions of the nonlinear component response under fire and blast loading in comparison with detailed nonlinear finite element analysis (Izzuddin [4]), as illustrated in Figure 2 for a simply supported beam subject to different levels of axial restraint.

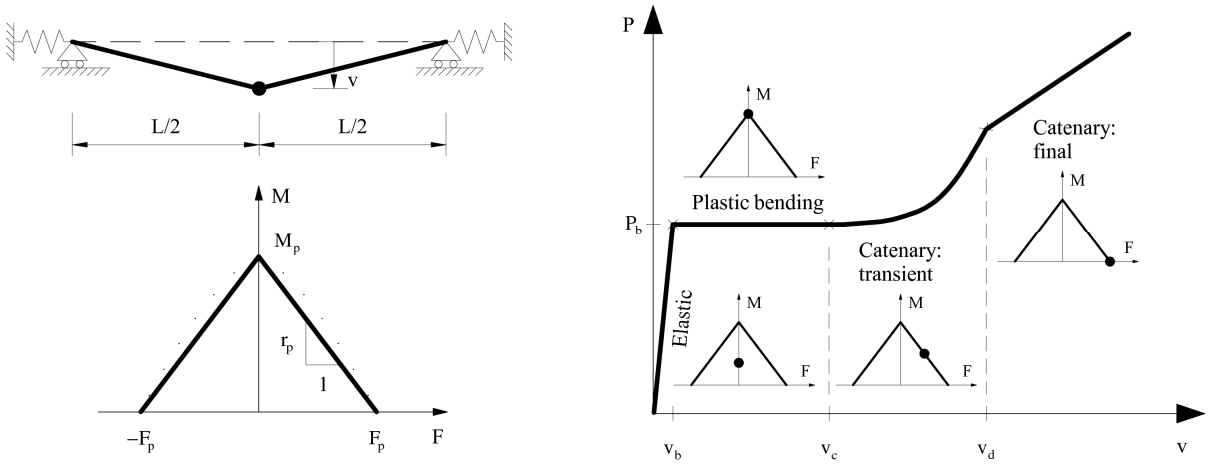

Figure 1: Simplified model for a simply supported beam accounting for plastic bending and catenary actions

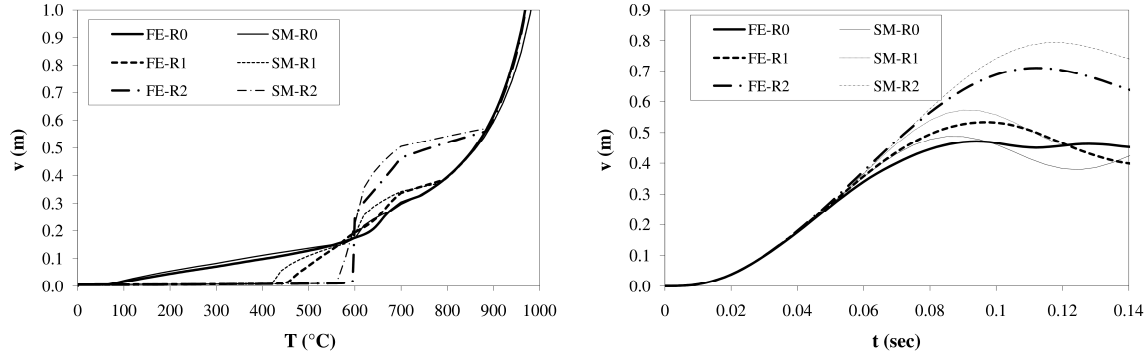

Figure 2: Response of simply supported beam for different axial restraints under fire (left) and blast (right)

3. Simplified Buckling Analysis Using Rotational Spring Analogy

A simplified method for buckling analysis of various types of structure was proposed by Izzuddin [5,6], which utilises a rotational spring analogy for the determination of the geometric stiffness matrix. An important benefit of this method is that it only requires familiarity with the principles of linear structural analysis, offering an intuitive framework for understanding the main parameters influencing the structural buckling response. In this method, the geometric stiffness can be obtained by including fictitious equivalent rotational springs for members with axial forces, where the spring stiffness ($k_\rho = F/L$) is negative/positive for compressive/tensile axial forces (F), respectively, L being the member length. Buckling can be conceived as a phenomenon that occurs when the geometric stiffness becomes sufficiently negative to overcome the positive material stiffness in a specific buckling mode. Besides this and other conceptual benefits (Izzuddin [5,6]), the computational power of the simplified method becomes apparent when the buckling load is approximated using an assumed mode (**U**), often obtained by applying to the linear structure a corresponding load pattern (**P**), for which the equivalent spring rotations (**ρ**) may be easily obtained. In this case, an approximate buckling load factor (λ_c) may be determined without assembling the geometric stiffness matrix, as follows [5]:

$$\lambda_c = -k_E \Big/ k_G^n = -\mathbf{U}^T\mathbf{P} \Big/ \sum_{i=1}^{m} \mathbf{k}_{\rho,i}^n \boldsymbol{\rho}_i^2 \tag{1}$$

The application of this simplified buckling analysis method to a plane frame is illustrated in Figures 3 and 4, where an approximation of the buckling load in accordance with (1) is obtained to with 1%.

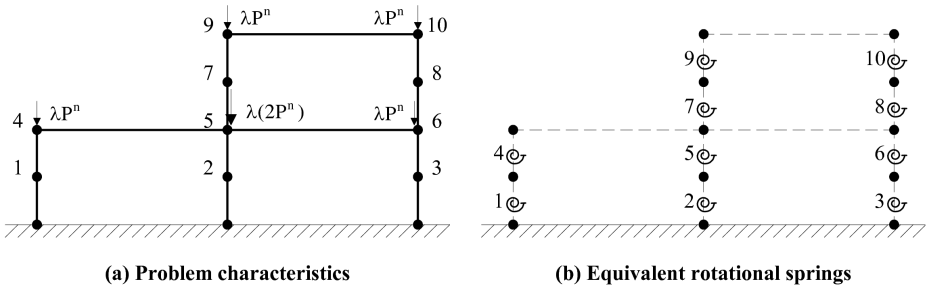

Figure 3: Geometric stiffness of frame using equivalent rotational springs

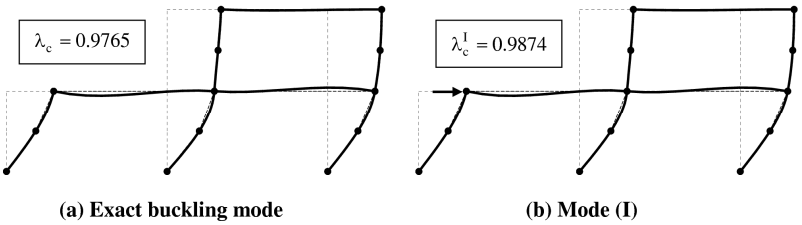

Figure 4: Buckling load prediction using an assumed mode with the rotational spring analogy

4. Simplified Progressive Collapse Assessment of Multi-Storey Buildings

Recent design codes of practice have included guidance for ensuring structural robustness (e.g. DoD [2]), aiming at the prevention of disproportionate/progressive collapse as a result of local damage. A typical local damage scenario is the sudden loss of a column in a multi-storey building (Figure 5), which could occur as a result of an extreme dynamic event, such as due to impact or blast. While consideration of the influence of such local damage on the overall structural system can be obtained with detailed nonlinear finite element analysis, this is often too complex for practical application.

A simplified multi-level framework has been recently developed (Izzuddin *et al.* [7], Vlassis *et al.* [8]), which allows progressive collapse assessment of multi-storey buildings to be undertaken at the lower levels of structural idealisation (Figure 5), depending on structural regularity and the feasibility of model reduction. Within this framework, the nonlinear static response of the considered component/sub-structure under gravity loading is first determined, and the failure displacement is established from ductility limits, typically governed for a steel framed building by the ductility supply in the connections.

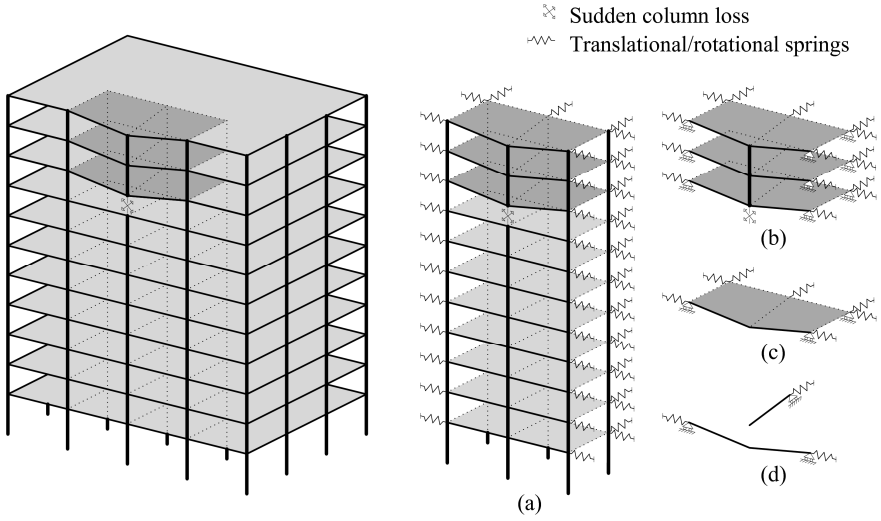

Figure 5: Multi-storey building subject to sudden column loss: levels of structural idealisation

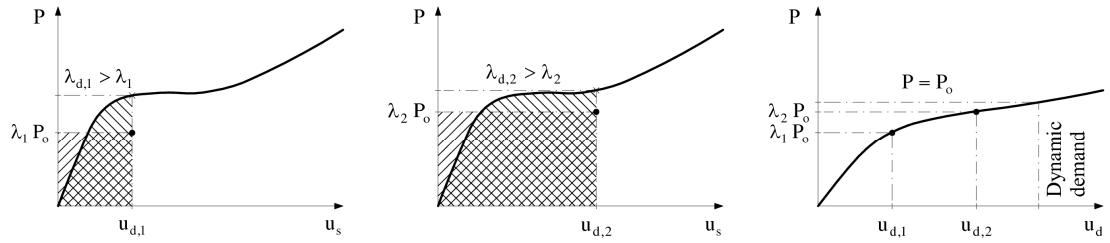

(a) Dynamic response ($P = \lambda_1 P_o$) (b) Dynamic response ($P = \lambda_2 P_o$) (c) Pseudo-static response

Figure 6: Simplified dynamic assessment under sudden column loss

In contrast with existing simplified design guidance, which suggests an excessively conservative dynamic load amplification factor of 2 to account for sudden column loss, a novel simplified dynamic assessment approach has been proposed (Izzuddin *et al.* [7]), which derives a maximum dynamic response from the previously determined nonlinear static response, leading to the concept of a *pseudo-static* dynamic response (Figure 6). In this respect, energy consrevation priicples are utilised, resulting in a dynamic load equal to the average static resistance over the range up to the maximum dynamic displacement (Figure 6), as expressed by:

$$P_n = \lambda_n P_o = \frac{1}{u_{d,n}} \int_0^{u_{d,n}} P \, du_s \tag{2}$$

For a specific level of gravity loading, the pseudo-static response provides the maximum dynamic displacement, which can be compared aganist the failure displacement, accounting for ductility supply, to define the progressive collapse limit state. The proposed simplified assessment method has been verified against detailed nonlinear finite element analysis (Vlassis *et al.* [8]), thus paving the way for its application in design practice.

5. Conclusion

The role of simplified modelling in nonlinear structural analysis is discussed, addressing a range of structural forms from individual components to overall systems. Three examples are presented which manifest the principal benefits of simplified modelling, including i) ease of application, ii) adequacy for preliminary assessment, iii) sufficiency in the presence of uncertainty in structure and/or load, and iv) explicit cause-and-effect formulation leading to enhanced understanding and appreciation of the main parameters influencing the nonlinear structural response

References

[1] Biggs JM. Introduction to Structural Dynamics, McGraw Hill, 1964.

[2] Department of Defense. Unified Facilities Criteria, Design of Buildings to Resist Progressive Collapse, UFC 4-023-03, Washington, DC, USA, 2005.

[3] Izzuddin BA. An Improved SDOF Model for Steel Members Subject to Explosion Loading - Generalised Supports and Catenary Action. Report Prepared for the Steel Construction Institute, 2001, U.K.

[4] Izzuddin BA. A simplified model for axially restrained beams subject to extreme loading. *International Journal of Steel Structures*, 2005; **5**:5:421-429.

[5] Izzuddin BA. Simplified buckling analysis of skeletal structures *Proceedings of the Institution of Civil Engineers, Structures and Buildings*, 2006; **159**:**4**:217-228.

[6] Izzuddin BA. Rotational spring analogy for buckling analysis. *Journal of Structural Engineering, ASCE*, 2007; **133**:**5**:739-751.

[7] Izzuddin BA, Vlassis AG, Elghazouli AY, Nethercot DA. Progressive collapse of multi-storey buildings due to sudden column loss – part I: simplified assessment framework. *Engineering Structures*, 2007; (doi:10.1016/j.engstruct.2007.07.011).

[8] Vlassis AG, Izzuddin BA, Elghazouli AY, Nethercot DA. Progressive collapse of multi-storey buildings due to sudden column loss – part II: application. *Engineering Structures*, 2007; (doi:10.1016/j.engstruct.2007.08.011).

Proceedings of the 6th International Conference on
Computation of Shell and Spatial Structures
IASS-IACM 2008: "Spanning Nano to Mega"
28-31 May 2008, Cornell University, Ithaca, NY, USA
John F. ABEL and J. Robert COOKE (eds.)

Limit analysis of slabs revisited with finite element models

Edward MAUNDER*, Angus RAMSAY

*School of Engineering, Computing & Mathematics, University of Exeter
Harrison Building, North Park Road, Exeter, EX4 4QF, UK
e.a.w.maunder@exeter.ac.uk

Abstract

The yield line method is a popular tool for the design of slabs, although it generates upper bound solutions which are inherently unsafe. The method based on finite element models composed of rigid triangular elements is revisited in this paper. The weak form of equilibrium used in the finite element approach is shown to provide the key to recovering strong forms of equilibrium that generate lower bound, and hence inherently safe, solutions. Two methods of recovery are described that lead to the determination of statically admissible moment fields in discrete elements, or in overlapping star patches of elements.

1. Introduction

Limit analyses to establish upper and lower bounds on collapse loads for slabs are potentially very useful in design, and in the context of reinforced concrete they are well known as Johansen's yield line method and Hillerborg's strip method. These methods are widely used as hand methods rather than as fully automated computational methods, and the exploitation of finite element methods have been relatively slow in development. Munro et al [8] proposed a yield line method based on a finite element model of rigid triangular elements with potential yield lines along the interfaces between elements. The virtual work equation, involving internal work of yield lines and external work of the loads, was used essentially to formulate primal and dual forms of linear programme (LP). The yield line method strictly provides an upper bound to the collapse load, and the method thereby suffers from being unsafe. However the use of yield line results may in practice be justified on the basis of engineering judgement, Kennedy et al [3] advocate hand methods and the safe use in practice for floor slabs, and Middleton [7] proposes a yield line method based on a library of some 27 yield line failure mechanisms for the assessment of bridge decks.

The yield line method normally provides no further information about moment fields beyond the yield line moments. However the method based on a finite element model provides much more information after the optimum collapse mechanism has been found. Then the normal bending moments along the sides of every element are quantified as also are a set of nodal forces, and together these quantities define a state of equilibrium for each element. Although such quantities may be used directly to define internal fields of moment, Fraeijs de Veubeke et al [2], and Krabbenhoft et al [4], they do not generally lead to continuity of torsional moments at element interfaces and thereby, in the opinion of the authors, do not fully satisfy equilibrium. However it is possible to recover moment fields that satisfy strong forms of equilibrium by further processing the side moments and nodal forces, and this paper outlines two approaches to the task of recovery. Then a complete field of statically admissible moments becomes available with which to establish a safe lower bound solution, i.e. both upper and lower bound solutions are derived from a yield line analysis.

The paper continues with, in Section 2, a review of the implementation of the yield line method using a finite element model and a numerical example; in Section 3, two methods to recover complete equilibrium of moment fields; and in Section 4, some conclusions.

2. Yield line method based on a finite element model

Following the terminology of Munro et al [8] the primal LP problem is posed with kinematic variables of nodal deflections and interface rotations, whereas the dual LP problem is posed with static variables of interface moments and the load factor. These LP problems were originally solved using a simplex algorithm, however the more recent experience of the authors has confirmed that much shorter solution times can be realized for relatively large problems based on fine meshes of elements when using primal-dual path following interior point algorithms.

Whichever algorithm is used duality ensures that a critical collapse mechanism is defined together with a complete set of normal bending moments acting on the sides of each element. Furthermore, since the virtual work equation in terms of the unit fan mechanism corresponding to each patch of elements sharing a common node (star patch) represents equilibrium of nodal forces, equilibrium of both elements and nodes is ensured. With reference to Figure 1(b), nodal forces $\left(\hat{\boldsymbol{F}}_1^{\boldsymbol{e}}, \hat{\boldsymbol{F}}_2^{\boldsymbol{e}}, \hat{\boldsymbol{F}}_3^{\boldsymbol{e}}\right)$ maintain element *e* in equilibrium with loads $\boldsymbol{f}^{\boldsymbol{e}}$ and side moments $\left(\boldsymbol{M}_1^{\boldsymbol{e}}, \boldsymbol{M}_2^{\boldsymbol{e}}, \boldsymbol{M}_3^{\boldsymbol{e}}\right)$, and equal and opposite nodal forces maintain each node in equilibrium as a free body. In the LP formulation, element loads are replaced with statically equivalent forces $\left(\boldsymbol{f}_1^{\boldsymbol{e}}, \boldsymbol{f}_2^{\boldsymbol{e}}, \boldsymbol{f}_3^{\boldsymbol{e}}\right)$.

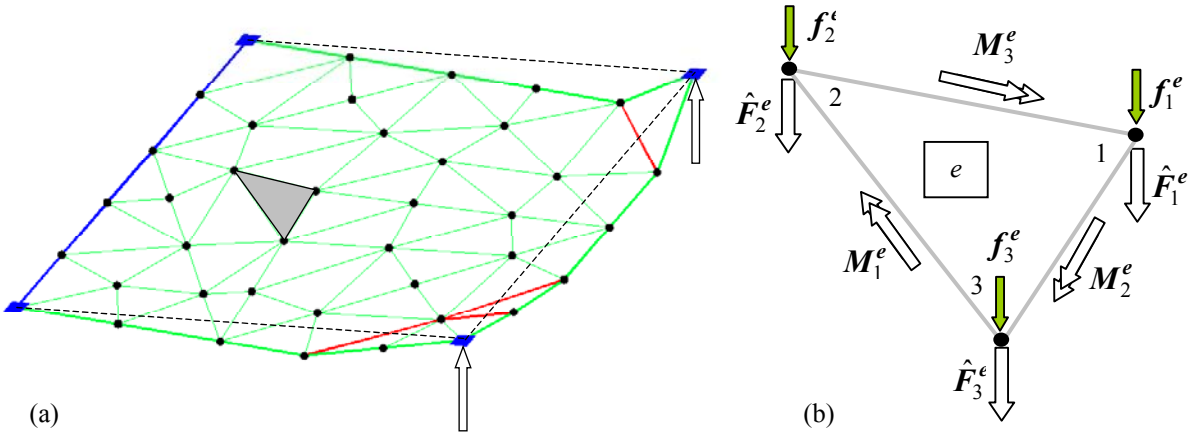

Figure 1: A finite element collapse mechanism and a weak form of element equilibrium.

The propped cantilever shown in Figure 1(a) serves to illustrate a yield line collapse mechanism determined from a finite element model. The slab is 10m square, fixed along one side and propped at the corners of the opposite side, and supports a uniformly distributed load. The yield moment is isotropic and equals 100kNm/m, sagging yield lines are shown in red and the hogging yield line along the fixed side is shown in blue. The corresponding collapse load equals 10.85kN/m^2. A typical element, shown in grey in Figure 1(a), is extracted as a free body in Figure 1(b).

3. Recovery of equilibrating moment fields for lower bounds

In this Section two methods for recovering strong forms of equilibrium in terms of statically admissible fields of moments and shear forces are outlined. Both methods make use of the concept of a star patch of elements, i.e. a patch of elements that share a common vertex or node. In topological terms the link of a star consists of those sides of the elements in the patch that are not connected to the vertex. Then a closed star has its vertex within a mesh and its link forms a closed circuit, whereas an open star has its vertex on the boundary of a mesh and its link forms a path with two separate ends.

3.1 Recovery element by element

Following the general method described by Ladeveze et al [5], co-diffusive equilibrating tractions on the sides of elements are derived from the nodal forces $\hat{\boldsymbol{F}}_{\boldsymbol{n}}^{\boldsymbol{e}}$.

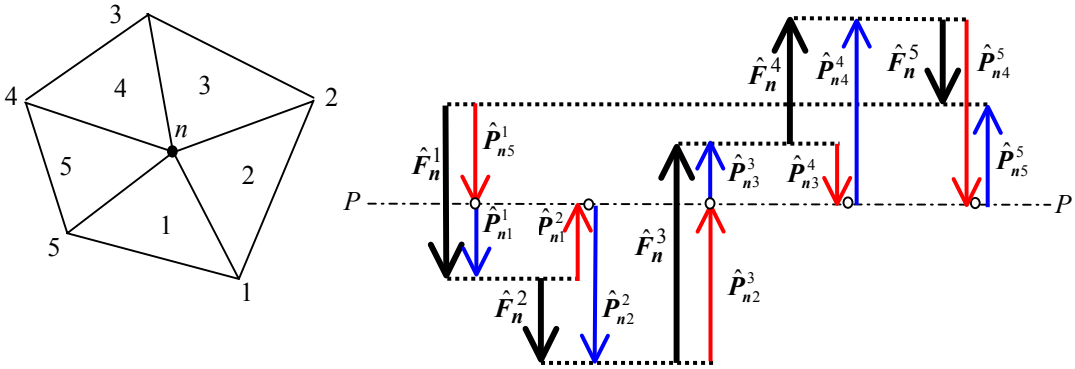

Figure 2: Resolution of nodal forces at a vertex of a closed star

The balanced set of forces $\hat{\boldsymbol{F}}_{\boldsymbol{n}}^{\boldsymbol{e}}$ for all elements e connected to node n form a closed polygon of forces as illustrated in Figure 2 for a closed star with 5 elements, when each force is considered in an anticlockwise sequence around the node. Since the nodal forces all act vertically, the force polygon is a 1-D form of a Maxwell force diagram. Thus to enable the components to be seen separately, the polygon has been stretched horizontally. A pole point P is introduced in order to resolve each force into 2 components, indicated by the red and blue vectors in Figure 2 where the pole point is stretched to the line P-P. Each nodal force is replaced by a pair of statically equivalent co-diffusive forces which are applied to the sides of the element adjacent to the node. In order to avoid unnecessarily large force components, the pole can be positioned to satisfy Equation (1).

$$\hat{\boldsymbol{F}}_{\boldsymbol{n}}^{\boldsymbol{e}} = \hat{\boldsymbol{P}}_{\boldsymbol{ni}}^{\boldsymbol{e}} + \hat{\boldsymbol{P}}_{\boldsymbol{nj}}^{\boldsymbol{e}} \quad \text{subject to minimization of} \quad \sum_{e}\left(\hat{\boldsymbol{P}}_{\boldsymbol{ni}}^{\boldsymbol{e}}\right)^2 \tag{1}$$

This condition corresponds to P positioned at the centroid of unit masses placed at the tails of each vector $\hat{\boldsymbol{F}}_{\boldsymbol{n}}^{\boldsymbol{e}}$. On the other hand, the pole position for open stars should account for known boundary tractions. The resultant shear forces and torsional moments acting at the midpoints of the sides of the element are replaced by uniform distributions of shear and moment tractions which are co-diffusive between elements. The final stage of recovery involves the analysis of each element to determine internal moment and shear fields that equilibrate with the tractions and loads. This generally requires the element to be replaced by a hybrid macro-element, as described by Maunder et al [6], of sufficient degree to equilibrate with the loads. In the event of an element with zero load, the macro-element can be of degree 1 with piecewise linear moment fields.

3.2 Recovery patch by patch

The basic idea in this method is similar to that currently being developed by Almeida et al [1]. Self-balanced load systems are defined on each star patch such that the superposition of all patch loads equals the distribution of loads as originally specified. Then each patch can be analysed separately to determine moment and shear fields that are statically admissible with the self-balanced loads. For closed stars the analysis is generally based on homogeneous static boundary conditions. The original loads are shared between patches using a partition of unity as a weighting function. A suitable function is conveniently provided by the deflections w that conform with a fan mechanism for a star having unit deflection at the internal vertex. When w is taken to represent deflections, the virtual work equation for a closed star can be expressed as in Equation (2).

$$0 = \int_{star} \boldsymbol{w} \cdot \boldsymbol{f} \cdot \boldsymbol{d\Omega} - \sum_{star} \int_{l} \theta_l \boldsymbol{m}_l \boldsymbol{dl} \tag{2}$$

where rotations θ_l conform with deflections w, and side moments m_l have been determined from a yield line analysis. Terms $(-\theta_l.m_l)$ are interpreted as fictitious line loads that equilibrate with loads $(w.f)$ in the transverse direction. The weighted loads $(w.f)$ sum to f at each point since w serves as a partition of unity, and the fictitious

loads on a side sum to zero for the patches corresponding to the 4 vertices belonging to the pair of elements for which the side is an interface. However these loads are generally unbalanced as regards moment equilibrium. A moment imbalance is then corrected by determining fictitious linear pressure distributions on each element of a patch such that the pressures sum to zero when all patches are superimposed. Further details of the determination of these fictitious pressures are in preparation for a future publication.

Having determined suitable load systems for each star, it remains to determine statically admissible stress fields separately for each star with homogeneous boundary conditions in general, using appropriate equilibrium finite element models. If the real loads involve uniformly distributed loads on elements, then the weighted loads on each star are piecewise linear, and the equilibrium elements need to be of minimum degree 3. This degree is also appropriate to equilibrate with the fictitious piecewise linear pressures as described above. Although cubic moment fields may be more problematic as regards checking against a yield criterion for moments, star patches of cubic elements are generally very stable (i.e. they do not contain spurious kinematic modes) apart from two easily identified configurations as discussed by Maunder et al [6]. These configurations can be stabilised if necessary by employing a form of local subdivision or mesh refinement to the equilibrium FE model.

4. Conclusions

The two methods of recovering lower bound solutions allow some choice of parameters, e.g. the position of the pole points *P* in the Maxwell force diagrams for the resolution of nodal forces; and the correction of unbalanced moments for star patches involves the determination of a solution of a network problem, this may also be based on a least squares procedure. These choices will affect the quality of the solutions, and they are currently under investigation. The nature of the lower bound may then be compared with the upper bound obtained from a yield line analysis and, if necessary, greater lower bounds may be sought by introducing hyperstatic moment fields as variables within the star patches and then solving a further non-linear optimization problem by mathematical programming. This problem is planned for future research by the authors.

Acknowledgement

The first author acknowledges with thanks the support provided by a Leverhulme Trust Emeritus Fellowship (EM/20218) during the preparation of this paper.

References

[1] Almeida JPM and Maunder EAW. A technique for recovery of equilibrium on star patches via a partition of unity. Submitted for presentation at *8th World Congress on Computational Mechanics*, Venice, 2008.

[2] Fraeijs de Veubeke BM and Sander G. An equilibrium model for plate bending. *International Journal of Solids and Structures* 1968; **4**: 447-468.

[3] Kennedy G and Goodchild CH. Practical Yield Line Design. The Concrete Centre; 2004.

[4] Krabbenhoft K and Damkilde L. Limit analysis based on lower-bound solutions and nonlinear yield criteria. In *Finite Elements: Techniques and Developments*, Topping BHV (ed). Civil-Comp Press: Edinburgh, 2000: 117-129.

[5] Ladeveze P, Maunder EAW. A general method for recovering equilibrating element tractions, *Comput. Methods Appl. Mech. Engrg.* 1996; **137**: 111-151.

[6] Maunder EAW and Moitinho de Almeida JP. The stability of stars of triangular equilibrium plate elements. Submitted for publication in the *International Journal for Numerical Methods in Engineering* in 2008.

[7] Middleton C. Generalised collapse analysis of concrete bridges. In *Morley Symposium on Concrete Plasticity and its Application*, Burgoyne C, Lees J, Middleton C. (eds). Cambridge University Engineering Department Technical Report CUED/D-STRUCT/TR.222, 2007; 193-205.

[8] Munro J, Da Fonseca AMA. Yield line method by finite elements and linear programming, *The Structural Engineer* 1978; **56B**, No 2: 37-44.

Proceedings of the 6th International Conference on
Computation of Shell and Spatial Structures
IASS-IACM 2008: "Spanning Nano to Mega"
28-31 May 2008, Cornell University, Ithaca, NY, USA
John F. ABEL and J. Robert COOKE (eds.)

Effects of boundary conditions on the non-linear long-term behaviour of spherical shallow concrete domes

Ehab HAMED*, Mark A. BRADFORD, R. Ian GILBERT

* Research Associate, Ph.D
Centre for Infrastructure Engineering and Safety, School of Civil and Environmental Engineering, The University of New South Wales, UNSW Sydney, NSW 2052, Australia
e.hamed@unsw.edu.au

Abstract

The design of shallow concrete domes is conducted under some level of uncertainty regarding the real boundary conditions. This paper aims to investigate the effects of the boundary conditions on the nonlinear behaviour of spherical shallow concrete domes, including the influence of the concrete creep and shrinkage. A theoretical model for the description of the full nonlinear long-term behaviour is presented. It is followed by a numerical study that investigates the short-term and long-term behaviour of concrete domes under different boundary conditions.

1. Introduction

The long-term behaviour of concrete structures, and the demand for strengthening and upgrading of existing structures because of extensive damage have been recognised and highlighted over the past two decades. Thin-walled concrete shells, and shallow spherical domes in particular, are structural components that are vulnerable to the effects of creep and shrinkage. While this structural system is effective from the perspectives of both structural and architectural design, many catastrophic failures of concrete domes have been reported worldwide (DPW-NSW [1]; Takeuchi et al. [2]). In most cases, the collapse was initiated by extensive cracking and deformations, which appeared to be a direct result of creep, shrinkage, and temperature effects (Moncarz et al. [3]). Thus, the long-term effects play important roles in the behaviour and structural safety of shallow, thin-walled concrete domes.

Creep and shrinkage effects generally increase the deformations of a concrete structure. However, while the deformations of shallow concrete domes along the meridian are partly restrained by the supporting ring, creep and shrinkage may also increase the compressive stresses in the dome while reducing the rise of the shallow dome. These two effects interact and they may produce localised damage or even eventuate in a state for which the arch may fail suddenly by so-called creep buckling. The dependence of the creep strains on the level of stress in the dome, and their interaction with shrinkage strains that may reduce or enhance the propensity of the dome to fail, make predicting the structural behaviour of the dome a challenging and difficult task.

Many efforts were devoted to study the nonlinear and buckling behaviour of domes (Hong and Teng [4]; Grigolyuk and Lopanitsyn [5]; Sharnappa and Sethuraman [6]). However, very little advanced research appears to have been reported on the long-terms effects in concrete shell structures, and in shallow concrete domes in particular. One of the most important influences affecting the long-term response of a shallow dome is the stiffness of the structural boundary restraints. The supporting system for a dome usually comprises of a prestressed or reinforced concrete edge ring or wall. The ability of the supporting system to constrain the deformations of the dome at the edges depends on its geometry, material, construction technique, and on its own long-term behaviour. In order to examine the safety of existing shallow concrete domes and to contribute to the effective and safe design of new concrete domes, an understanding of the influences of the boundary conditions on their non-linear long-term behaviour is essential. This paper aims to provide insights into these effects.

2. Theoretical model

The sign conventions of an axisymmetric spherical shallow concrete dome are shown in Fig. 1. The variational principle is used for the derivation of the governing equations, which for brevity is not presented here.

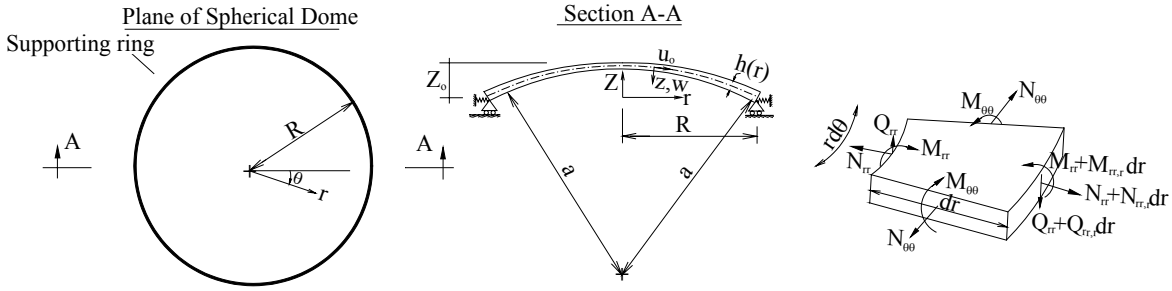

Figure 1: Geometry, sign conventions, and internal forces and moments

Following the Love-Kirchhoff assumptions and Donnell's theory for shallow shells, and assuming an axisymmetric distribution of the long-term strains, the time-dependent nonlinear mechanical radial and circumferential strains in the shallow dome take the following form (Gilbert [7]; Brushand and Almorth [8]):

$$\varepsilon_{rr}(r,z,t) = u_{o,r}(r,t) - \frac{w(r,t)}{a} + \frac{1}{2}w_{,r}^{2}(r,t) - z w_{,rr}(r,t) - \varepsilon_{c}(r,z,t) - \varepsilon_{sh}(r,z,t) \tag{1}$$

$$\varepsilon_{\theta\theta}(r,z,t) = \frac{u_{o}(r,t)}{r} - \frac{w(r,t)}{a} - \frac{z}{r}w_{,r}(r,t) - \varepsilon_{c}(r,z,t) - \varepsilon_{sh}(r,z,t) \tag{2}$$

where v and w are the axisymmetric tangential and perpendicular deformations respectively, ε_{cr} and ε_{sh} are the creep and shrinkage strains respectively, and $(\,)_{,r}$ denotes a derivative with respect to r. The shrinkage strain and the creep coefficient are determined based on the recommendations of the ACI Committee-209 [9].

The nonlinear equilibrium equations are formulated using the variational principle along with the kinematic relations (Eqs. (1-2)), and take the following form:

$$-\left(rN_{rr}\right)_{,r} + N_{\theta\theta} - q_{r}r = 0 \quad ; \quad \frac{r}{a}\left(N_{rr} + N_{\theta\theta}\right) + \left(rQ_{rr}\right)_{,r} + q_{z}r = 0 \tag{3,4}$$

$$Q_{rr} = \frac{rN_{r}w_{,r} + \left(rM_{rr}\right)_{,r} - M_{\theta\theta}}{r} \tag{5}$$

where N_{rr} and $N_{\theta\theta}$ are the radial and the circumferential axial forces, M_{rr} and $M_{\theta\theta}$ are the radial and the circumferential bending moments, Q_{rr} is the radial shear force, and q_r and q_z are axisymmetric external distributed tangential and perpendicular surface loads respectively.

The boundary conditions are:

$$\lambda N_{rr} = -\xi k v \quad \text{or} \quad u_{o} = u_{p} \tag{6}$$

$$\lambda M_{rr} = M_{e} \quad \text{or} \quad w_{,r} = w_{p,r} \tag{7}$$

$$\lambda Q_{rr} = V_{e} \quad \text{or} \quad w = w_{p} \tag{8}$$

where V_e and M_e are external loads and bending moments at the edges; u_p and w_p are prescribed deformations; $\lambda = 1$, $\xi = 1$ where $r = R$ and $\lambda = -1$, $\xi = 0$ where $r = 0$. k is the extensional stiffness of the supporting ring.

Following Hooke's law and the kinematic relations (Eqs. (1-2)), the constitutive relations take this form:

$$N_{rr} = \frac{A(t_{o})}{1 + \chi(t,t_{o})\phi(t,t_{o})}\left[u_{o,r} - \frac{w}{a} + \frac{1}{2}w_{,r}^{2} + \nu\left(\frac{u_{o}}{r} - \frac{w}{a}\right) - \varepsilon_{sh}(1+\nu)\right] \tag{9}$$

$$N_{\theta\theta} = \frac{A(t_o)}{1+\chi(t,t_o)\phi(t,t_o)}\left[\frac{u_o}{r} - \frac{w}{a} + \nu\left(u_{o,r} - \frac{w}{a}\right) - \varepsilon_{sh}(1+\nu)\right] \tag{10}$$

$$M_{rr} = -\frac{D(t_o)}{1+\chi(t,t_o)\phi(t,t_o)}\left[w_{,rr} + \frac{\nu}{r}w_{,r}\right] \quad ; \quad M_{\theta\theta} = -\frac{D(t_o)}{1+\chi(t,t_o)\phi(t,t_o)}\left[\frac{1}{r}w_{,r} + \nu w_{,rr}\right] \tag{11,12}$$

where $\chi(t,t_o)$ is the aging coefficient, $\phi(t,t_o)$ is the creep coefficient (t_o is the time at first loading in days), $A(t_o)$ and $D(t_o)$ are the in-plane and bending rigidities of the dome shell at the age of loading, ν is the Poisson's ratio. Substitution of the constitutive relations (Eqs.(9-12)) into the equilibrium equations (Eqs. (3-5)) yields a set of nonlinear differential equations in terms of the unknown deformations (u,w) and the unknown shear force (Q_{rr}). The multiple shooting method along with the arc-length continuation technique are used here for the solution of the governing equations, together with their boundary conditions.

3. Numerical study

The geometry of the examined dome, which is subjected to its self-weight plus a uniform sustained load, is shown in Fig. 2. The modulus of elasticity is taken as $E = 28.6 \times 10^3$ MPa assuming $t_o = 28$ days. Three cases are examined. The first case describes a simply supported dome; the second case describes a fixed-ended dome; and the third case describes a dome that is supported by a flexible ring, which is modeled as a horizontal spring.

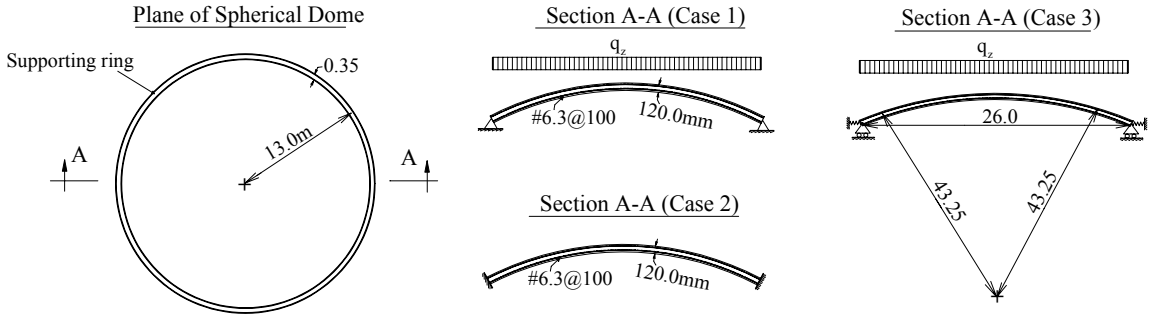

Figure 2: Geometry and structural scheme of a shallow dome with different boundary conditions

The nonlinear short-term equilibrium paths of the dome appear in Fig. 3a. The results reveal that the nonlinear behaviour of the dome is characterized by a limit point type of behaviour. The results also show that the limit load of the simply supported dome is almost the same as that of the fixed dome and equals about 70 times the self-weight (with a normalized deflection of 0.045 its rise). However, the limit load of the dome with a flexible ring is about 37% of that for the simply supported dome (26 times the self-weight), while its limit vertical deflection is more than three times that of the simply supported dome (0.14 its rise).

The time-dependent behaviour of the dome with different boundary conditions appears in Fig. 3b. The simply supported and fixed domes are subjected to a sustained load equal to 0.4 times their limit load, while the dome with flexible ring is subjected to a sustained load of 0.55 times its limit load. It is seen that the time to cause buckling is $t_{cr} = 276$ days after first loading for the simply supported dome, $t_{cr} = 330$ days for the fixed dome, and $t_{cr} = 309$ days for the dome with flexible supporting ring (see Fig. 3b). Thus, although the load carrying capacity of the simply supported and fixed domes is greater than that of the dome with flexible ring, the nonlinear behaviour of the simply supported and fixed domes is more sensitive to the long-term effects. These preliminary results reveal the very important role the boundary conditions play in the nonlinear long-term response of shallow concrete domes.

The behaviour of the dome with a flexible supporting ring at three different times (namely: $t = t_o = 28$, $t = 100$, $t = 200$ days) is depicted in Fig. 4. The behaviour at $t = t_o$ corresponds to the instantaneous response of the dome without any long-term effects. Fig. 4a shows that the time-dependent effects significantly increase and modify the distribution of the perpendicular deformations with time. This effect, along with the variation of the radial forces with time (Fig. 4b), provide quantitative explanation for the creep buckling behaviour of the shallow concrete dome (Fig. 3).

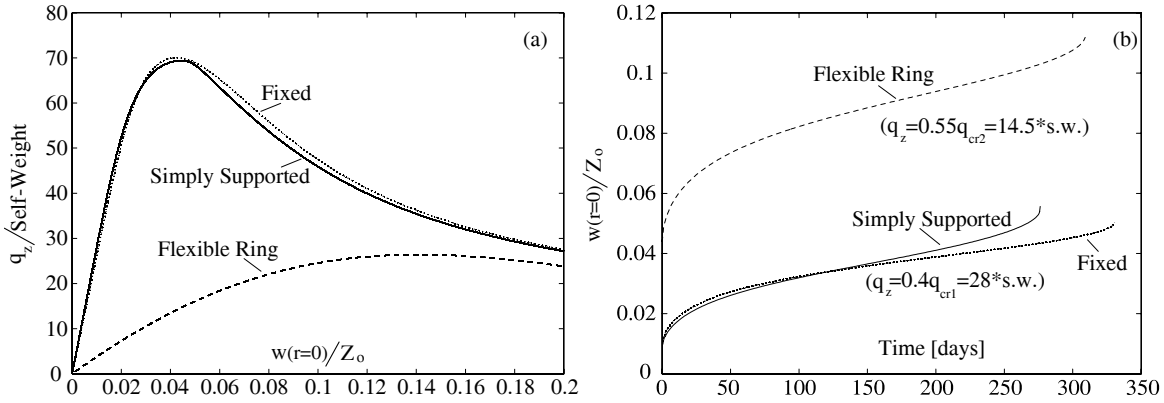

Figure 3: Nonlinear behaviour: (a) Short-term; (b) Long-term

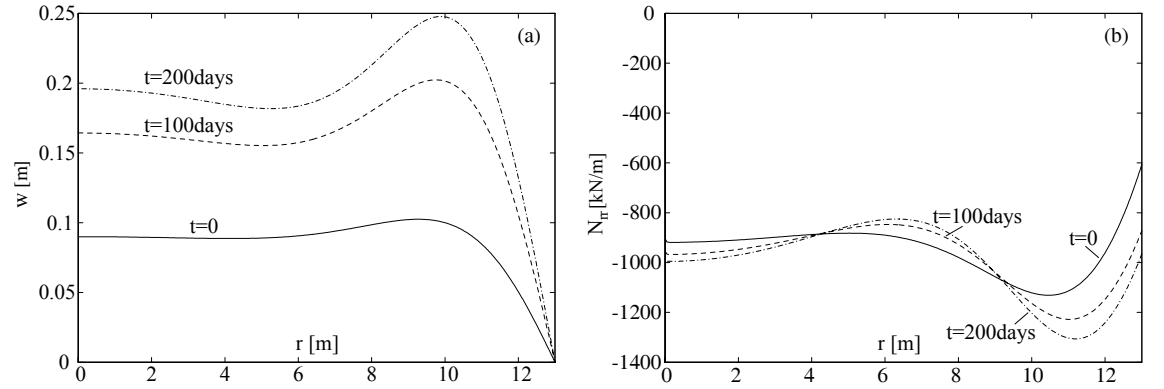

Figure 4: Long-term response at three different times

Acknowledgement

The work reported in this paper was supported by the Australian Research Council (ARC) through a Discovery Project awarded to the second and third authors.

References

[1] DPW-NSW, *Construction of Binishell reinforced concrete domes*, New South Wales, Australia/Department of Public Works, 1978.

[2] Takeuchi, H, Taketomi, S, Samukawa, S and Nanni, A. Renovation of Concrete Water Tank in Chiba Prefecture, Japan. *Practice Periodical on Structural Design and Construction ASCE* 2004, **9**(4): 237-241.

[3] Moncarz, PD, Griffith, M and Noakowski, P. Collapse of a Reinforced Concrete Dome in Wastewater Treatment Plant Digester Tank. *Journal of Performance of Constructed Facilities ASCE* 2007, **21**(1): 4-12.

[4] Hong, T and Teng, JG. Non-Linear Analysis of Shells of Revolution under Arbitrary Loads. Computers and Structures 2002, **80**(18-19): 1547-1568.

[5] Grigolyuk, EI and Lopanitsyn, YA, The Axisymmetric Postbuckling Behaviour of Shallow Spherical Domes. *Journal of Applied Mathematics and Mechanics PMM*, **66**(4): 605-616.

[6] Sharnappa, Ganesan, N and Sethuraman, R. Buckling and Free Vibrations of Sandwich General Shells of Revolution with Composite Facing and Viscoelastic Core under Thermal Environment using Semi-Analytical Method. *CMES-Computer Modeling In Engineering & Sciences*, **18**(2): 121-144.

[7] Gilbert, RI. Time Effects in Concrete Structures, Elsevier Science Publishers B.V., Amsterdam, 1988.

[8] Brush, DO and Almorth, BO, *Buckling of Bars, Plates, and Shells*, McGraw-Hill, Inc., New-York.

[9] ACI Committee-209. Prediction of Creep, Shrinkage, and Temperature Effects in Concrete Structures. American Concrete Institute (ACI), Detroit, USA, 1982.

Proceedings of the 6th International Conference on
Computation of Shell and Spatial Structures
IASS-IACM 2008: "Spanning Nano to Mega"
28-31 May 2008, Cornell University, Ithaca, NY, USA
John F. ABEL and J. Robert COOKE (eds.)

A local failure model for shallow spherical concrete domes subjected to uniform external radial pressure

Zhen-Tian CHANG, Mark A. BRADFORD*, R. Ian GILBERT

* Scientia Professor and corresponding author
Centre for Infrastructure Engineering and Safety
School of Civil and Environmental Engineering
The University of New South Wales
UNSW Sydney, NSW 2052, Australia
Email: m.bradford@unsw.edu.au

Abstract

Many thin shallow concrete shells have experienced structural collapses during and subsequent to their erection, and so translating theory into practice in such a way as to maintain their safety and integrity is essential. Very few experimental investigations have been reported of shallow concrete shells or domes that allow for the effects of geometric and material non-linearities and imperfections to be identified, despite this information being much-needed to validate sophisticated numerical treatments. Classical shell theories for axisymmetric domes without initial imperfections predict a global buckling mode, but observations from experimental tests show that failure in concrete domes is usually localised within a small region at a load significantly less than the theoretical buckling load. The authors are currently investigating the non-linear behaviour of axisymmetric domes, both experimentally and theoretically, as part of a research project at The University of New South Wales. As part of this study, the present paper reports a local yield-line failure model for evaluating the failure pressure of shallow spherical concrete domes subjected to externally applied uniform radial pressure. A calibration has been undertaken between the analytical results and the results from work at the State University of Ghent and at Massachusetts Institute of Technology, with excellent correlation being obtained. This model forms an efficient means of designing shallow reinforced concrete spherical domes in practice, and for inclusion in sophisticated numerical models of dome strength behaviour.

1. Introduction

Studies of the elastic stability of spherical shells form a component of fundamental engineering mechanics research, and contributions to this topic have been numerous over the decades. The critical buckling pressure p_{cr} for spherical shell was derived first in 1915 by Zoelley [1], based on linear elastic theory and an axisymmetric buckling pattern. This classical theoretical result is expressed as

$$p_{cr} = \frac{2}{\sqrt{3(1-\nu^2)}} \cdot \frac{Et^2}{R^2}, \tag{1}$$

where E is the elastic modulus, R the radius and t the thickness. The same result was obtained by van der Neut [2] who assumed an asymmetric buckling pattern. Nevertheless, experimental values reported by various investigators were found to be significantly lower than the theoretical buckling pressure. In order to explain the discrepancy between the linear buckling load and test results, large deflection (non-linear) theory has been used and initial imperfections have been taken into account in the analysis of spherical shells and caps. Huang [3] presented a numerical study of the problem of unsymmetrical buckling of thin shallow spherical shells, in which

the derived buckling pressure is based on the initiation of unsymmetrical deflections with an integer n indicating the number of circumferential full-waves in the unsymmetrical mode. This unsymmetrical buckling pressure reduced the gap between theory and experiments, but it is still higher than the experimental results. The presence of initial imperfections is presumed to be the source of this discrepancy.

Most theoretical and experimental studies of spherical shells or domes are based on linear elastic material behaviour and very few of them dealt with the effects of non-linear material behaviour such as cracking and creep. Among experimental investigations, very few have been reported on spherical concrete or mortar domes.

The most comprehensive experimental study of concrete/mortar domes was undertaken by Vandepitte and his colleagues from 1970 to 1985 at the State University of Ghent [4]. A total of 75 spherical model domes made of micro-concrete were tested over this period; 34 domes were tested by rapid loading under uniform radial pressure until failure and the other 41 were tested under a constant radial long-term pressure to study their creep buckling behaviour. It was found in their experimental tests that all of the micro-concrete domes failed in the same manner with a circular local area of the shell being "punched out". The average mean diameter of the punched out disks was equal to $2.76\sqrt{(Rt)}$, where R is the radius of the dome and t its thickness. The experimental buckling pressure in the rapid loading tests were found to be much lower than the classical critical pressure given by Equation (1), with an average pressure ratio of 0.46 of the theoretical value for 23 domes supported on non-prestressed steel rings and an average ratio of 0.53 for 11 domes supported on prestressed steel rings. During the long-term pressure testing, a number of full waves (n = 9) were detected in the circumferential direction of some domes. This number of full waves in the circumferential direction correlated well with that predicted by Huang [3] based on the geometric parameters of the Ghent domes. This observation provided support to Huang's unsymmetrical buckling mode hypothesis.

Another experimental investigation of two spherical mortar domes was reported by Litle *et al.* [5] in 1970 at Massachusetts Institute of Technology. The experimental buckling loads were also found to be only approximately 40% of the theoretical value, and so are in accord with Vandepitte's results.

2. Local yield-line failure model for shallow spherical concrete domes

The Ghent dome tests [4] demonstrated that all the micro-concrete domes failed in the same manner with an almost circular area of the shell being punched out. The localised area of failure of the dome was reported to be at one of the dents that occurs when the shell develops an unsymmetrical circumferential wave-form deformation; this is hypothesised by the present authors to be similar to a concrete slab subjected to two-way bending and membrane actions in both directions. The process of dome failure was found to start around the perimeter of a buckling dent, where the concrete is cracked on the convex side of the dome, followed by the concrete crushing on the concave side along the perimeter as well as along a number of radiuses of the dent. Such a local dome failure pattern is hypothesised to be similar to the yield line failure mechanism of a reinforced concrete (RC) slab of circular or regular shape under uniform load, as shown in Figure 1.

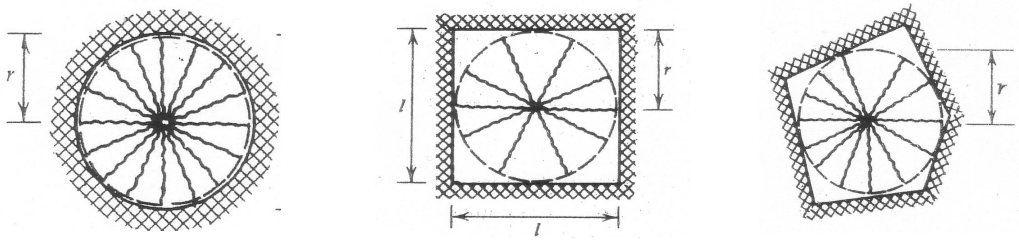

(a) **(b)** **(c)**

Figure 1: Uniformly loaded slabs with a circular and conical yield line patterns

Using rigid plastic yield line theory for a circular failure pattern, the ultimate uniform load per unit area w_u can be expressed as (Park and Gamble [6])

$$w_u = \frac{6\left(m'_u + m_u\right)}{r^2}, \tag{2}$$

where m'_u and m_u are the ultimate negative and positive bending strengths per unit width of the reinforced concrete slab, and r is the radius of the circle.

The authors propose the use of a yield line model for evaluating the ultimate radial pressure that causes a local failure of a concrete shallow spherical dome. However, while the ultimate bending strength in RC slabs can be calculated by well-known semi-empirical formulae based on experimental results, the ultimate bending strength of a plain concrete section without reinforcement needs to be derived under combined bending and compression.

Chen [7] has examined the moment-curvature relationship of a plain concrete section either under pure bending or under combined bending and compression, and he concluded that limit analysis can be applied to plain concrete in the presence of axial thrust for which gradual cracking of the section takes place.

In this paper, in order to calculate the ultimate bending strength per unit width of a plain concrete shell section, the following assumptions are made:

(a) the membrane forces in the dome shell under a uniform radial pressure p may be calculated from membrane theory as $N_\phi = N_\theta = 0.5\,pR$;

(b) plane sections remain plane after deformation;

(c) the tensile strength of the concrete may be neglected; and

(d) the stress-strain relationship for concrete in the compressive zone can be expressed by the equations

$$\frac{\sigma_c}{f_{cm}} = \begin{cases} 2\left(\dfrac{\varepsilon}{\varepsilon_0}\right) - \left(\dfrac{\varepsilon}{\varepsilon_0}\right)^2 & \varepsilon \le \varepsilon_0 \\ 1 - 0.15\left(\dfrac{\varepsilon - \varepsilon_0}{\varepsilon_u - \varepsilon_0}\right) & \varepsilon_0 < \varepsilon \le \varepsilon_u \end{cases} \tag{3}$$

where $\varepsilon_u = 0.003$ is the maximum compressive strain at the extreme fibre of a section at the ultimate, $\varepsilon_0 = 0.002$ is the strain corresponding to the peak stress f_{cm} in the stress-strain curve and f_{cm} is taken as 93% of the concrete compressive strength f'_c, based on the results of Hognestad *et al.* [8] for $f'_c = 50$ MPa.

Therefore, using the two equilibrium conditions that $\sum N_n = 0$ and $\sum M_n = 0$, the ultimate positive or negative moment strength per unit width, m^+_u or m^-_u can be derived for a cracked plain concrete section perpendicular to the n direction and subjected to combined bending and compression. The ultimate external uniform radial pressure w_u on a shallow spherical concrete dome based on the local yield-line failure model is then calculated from Equation (2), where r is taken as half of $2.76\sqrt{(Rt)}$, as the average radius of the punched out circle in the Ghent concrete dome tests.

3. Comparison between experimental and analytical results

The experimental failure loads p_u of the Ghent and MIT micro-concrete dome tests have been compared with the classical theoretical elastic buckling pressure p_{cr} given by Equation (1) and the analytical result w_u obtained using Equation (2) based on the local yield-line failure model. The overall comparisons between the experimental value p_u and theoretical result p_{cr} or the yield-line model result w_u are shown in Table 1.

It can be seen from the table that the test results are generally much lower than the linear elastic buckling pressure of Equation (1), and that excellent correlation exists between the experimental test results and the calculated values based on the local yield-line failure model, despite the edge restraint conditions being somewhat different in these test groups. Therefore, this model affords a convenient means of handling

imperfections and edge restraint conditions and it forms an efficient means of designing shallow reinforced concrete spherical domes in practice.

Table 1: Comparison of experimental and theoretical results

	Micro-concrete spherical domes tested at Ghent		Mortar domes tested at MIT
Edge Support	Steel ring-beam	Prestressed steel ring-beam	Clamped edges
No. of Shells	23	11	2
Average p_u / p_{cr}	0.459	0.530	0.402
Coefficient of variation	8.5%	15.1%	17.1%
Average p_u / w_u	0.966	0.965	1.005
Coefficient of variation	6.5%	4.7%	2.7%

4. Discussion

Yield line theory is an upper bound method for the limit state analysis of reinforced concrete slabs. However, the results of this study show that the local yield-line failure model provides an excellent estimation of the experimental failure loads of shallow spherical concrete/mortar domes. While an unsymmetrical buckling mode with circumferential waves was detected in the Ghent tests, the buckling pressure predicted by Huang's method [3] is still much higher (by approximately 30% to 40%) than the actual dome failure pressure, and this may be attributed to the material failure, as described by this local yield-line model, during buckling of the dome. This study deals with the concrete dome failure problem in a different light to those based on elastic instability, and affords a means of inclusion of material failure into numerical elastic non-linear pre-buckling analyses of shallow thin-walled concrete domes.

References

[1] Zoelley, R., Uber ein Knickproblem an der Kugelschale. *Thesis*, Zurich, 1915.

[2] Van der Neut, A., The elastic stability of the thin-walled sphere. *Thesis*, Delft, 1932.

[3] Huang, N. C. Unsymmetrical buckling of thin shallow spherical shells, *Journal of Applied Mechanics*, Sep., 1964.

[4] Vandepitte, D. and Lagae, G. Buckling of spherical domes made of micro-concrete and creep buckling of such domes under long-term loading, *Inelastic Behaviour of Plates and Shells*, IUTAM Symposium, Rio de Janeiro, Brazil, Aug., 1985.

[5] Litle, W. A., Forcier, F. J. and Griggs, P. H. Can plastic models represent the buckling behaviour of reinforced concrete shells?, ACI SP-24, *Models for Concrete Structures*, Detroit, Michigan, 1970.

[6] Park, R. and Gamble, W. L. Reinforced Concrete Slabs, John Wiley & Sons, 1980.

[7] Chen, W. F. Plasticity in Reinforced Concrete, McGraw-Hill Book Company, 1982.

[8] Hognestad, E., Hanson, N.W. and McHenry, D. Concrete stress distribution in ultimate strength design, *Journal of the American Concrete Institute*, Vol. 52, No. 6, Dec., 1955, pp. 455-479.